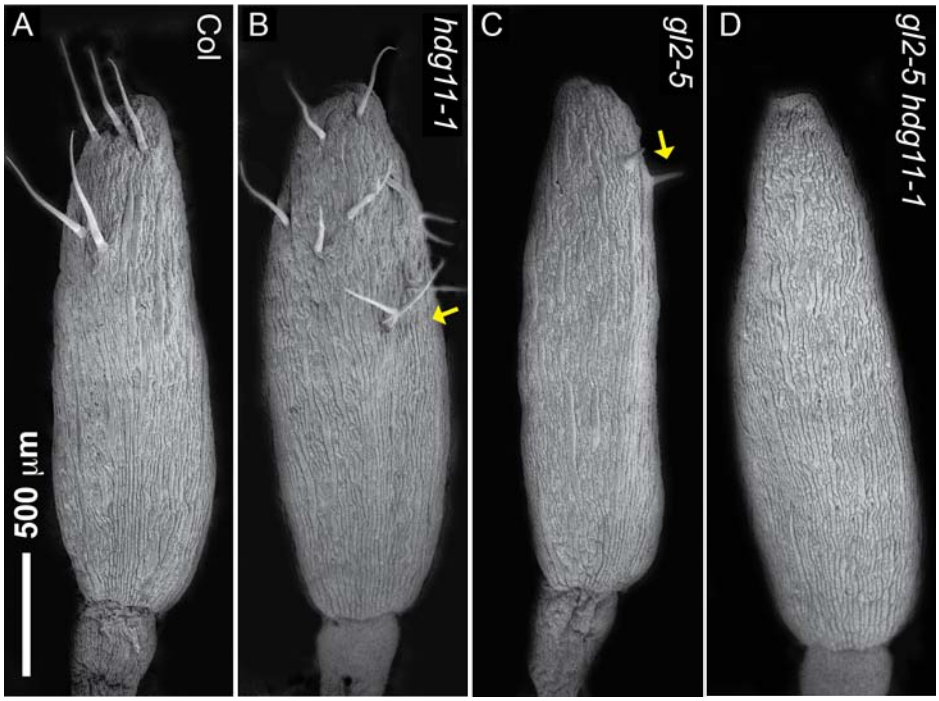

Supplemental Figure 1. Trichomes on sepals from *Arabidopsis* flowers. (A-D) Scanning electron micrographs (SEM) of sepals. In comparison to **(A)** wild-type Col in which unbranched trichomes form on sepals, **(B)** *hdg11-1* sepals display both unbranched and branched trichomes (arrow). **(C)** *gl2-5* mutant sepals display fewer trichomes that are aborted in differentiation (arrow), while **(D)** *gl2-5 hdg11-1* double mutants lack visible trichomes.

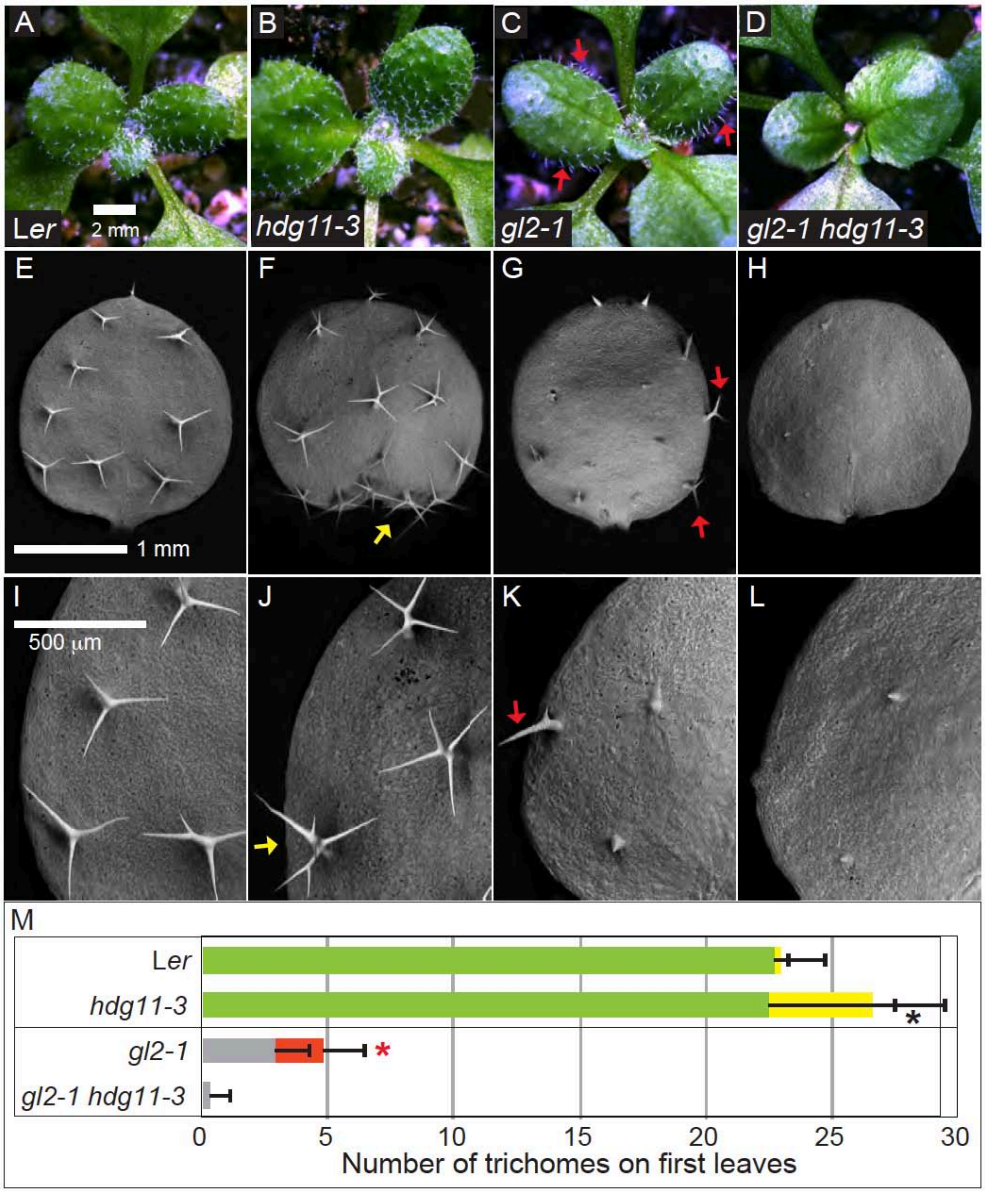

Supplemental Figure 2. *gl2-1 hdg11-3* double mutants from the L*er* ecotype exhibit enhanced trichome differentiation defects. (A-D) Rosettes from 3-week-old plants. **(A)** L*er* wild-type and **(B)** *hdg11-3* plants display evenly-spaced trichomes on young leaves. **(C)** *gl2-1* plants exhibit fewer trichomes. Arrows mark trichomes on leaf margins. **(D)** *gl2-1 hdg11-3* plants have glabrous leaf surfaces. **(E-L)** Scanning electron micrographs of first leaves reveal trichome morphology details. **(E,I)** L*er* wild-type trichomes exhibit a maximum of 3-4 branches, while **(F,J)** *hdg11-3* leaves exhibit some trichomes with ectopic branching (arrows). **(G,K)** *gl2-1* leaves exhibit trichome branching (arrows) at leaf edges. In comparison, **(H,L)** *gl2-1 hdg11-3* trichomes appear smaller and undifferentiated. **(M)** Quantification of trichomes and trichome branching on first leaves as described in Figure 2U. Positive error bars indicate standard deviations for n $\geq$ 20 plants. Asterisks indicate significant differences in trichome branching (Two-tailed *t*-test, P < 0.00001).

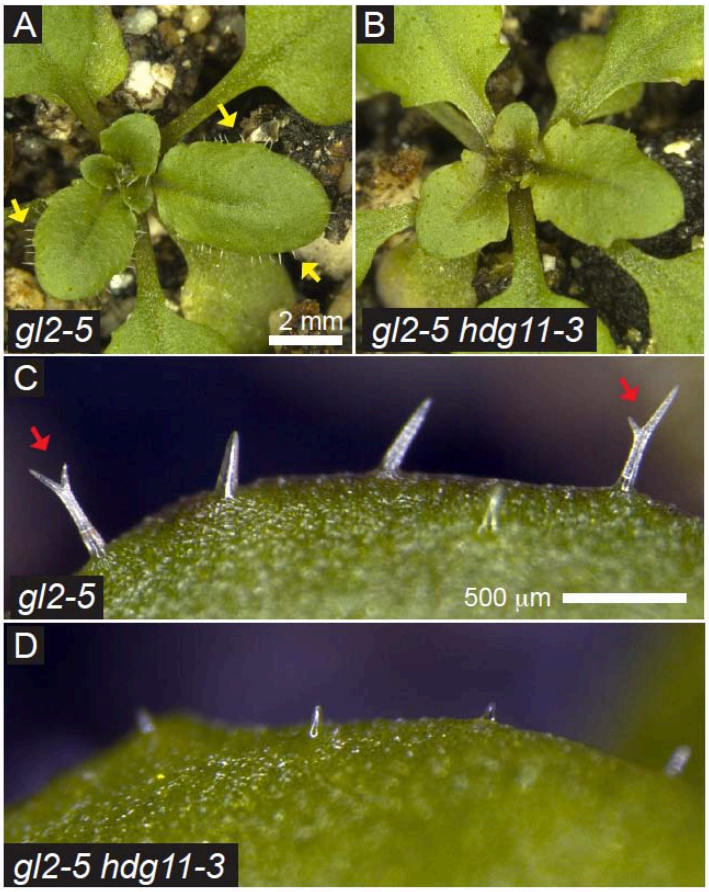

Supplemental Figure 3. Trichome phenotype of *gl2-5 hdg11-3* mutants. F3 progeny from a cross between *gl2-5* plants harboring the *ProGL2:EYFP:GL2* transgene and *hdg11-3* plants were analyzed for phenotypes. *gl2-5* single mutant segregants from an F2 line lacking EYFP expression were compared to the *gl2-5 hdg11-3* double mutants. **(A,B)** Rosette phenotypes of **(A)** *gl2-5* and **(B)** *gl2-5 hdg11-3* reveal trichomes on leaf margins of *gl2-5* plants (arrows) but few or no trichomes on leaf margins of the double mutant. **(C,D)** Magnification of leaf margins shows that **(C)** *gl2-5* plants display some trichomes with branching (red arrows), while **(D)** *gl2-5 hdg11-3* leaves display smaller trichomes that lack branching.

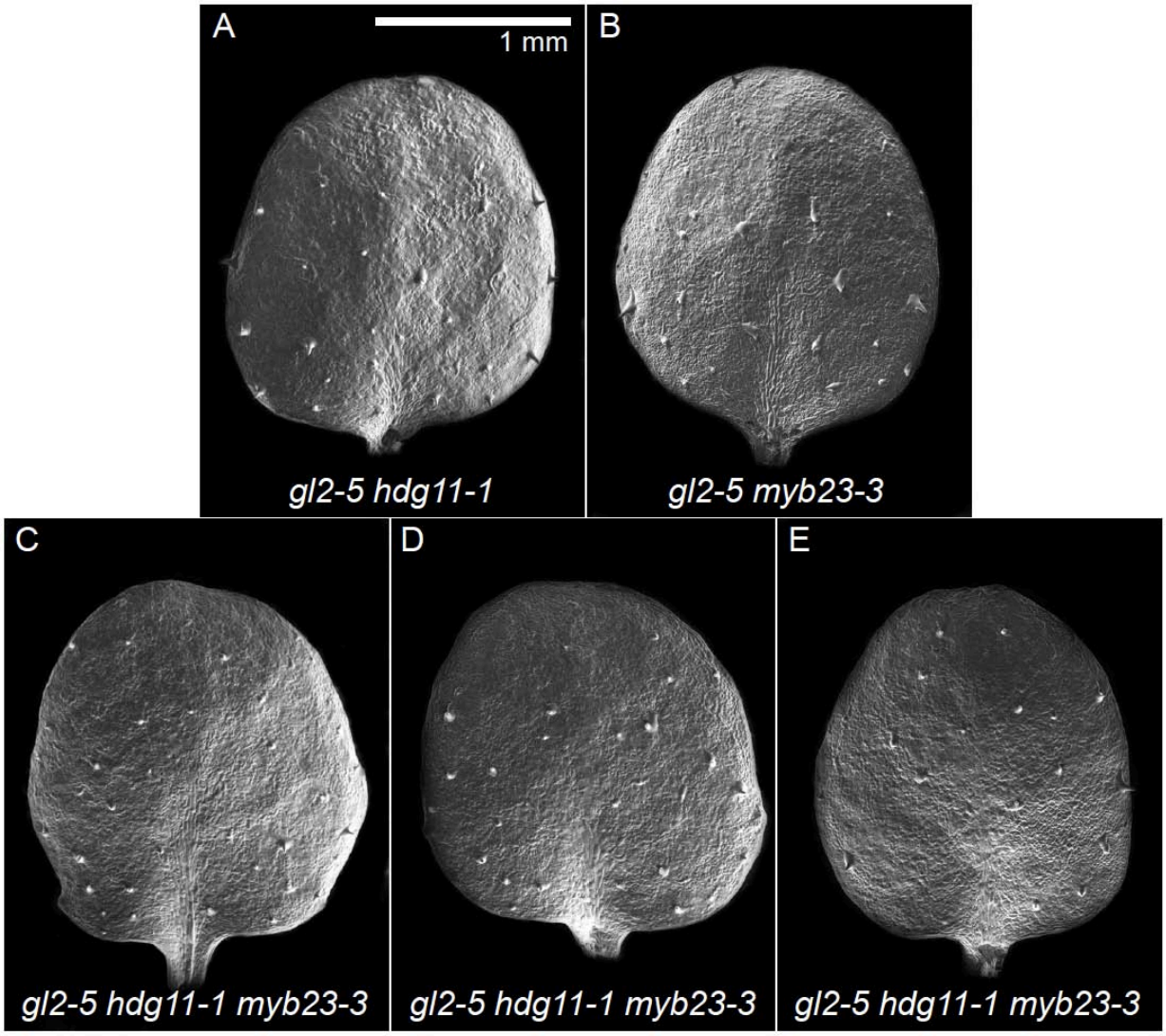

Supplemental Figure 4. Trichomes on first leaves of the *gl2-5 hdg11-1 myb23-3* triple mutant. (A-E) Scanning electron micrographs of first leaves. The double mutants **(A)** *gl2-5 hdg11-1* and **(B)** *gl2-5 myb23-3* display trichome differentiation defects that are similar to those observed for **(C-E)** *gl2-5 hdg11-1 myb23-3* triple mutants.

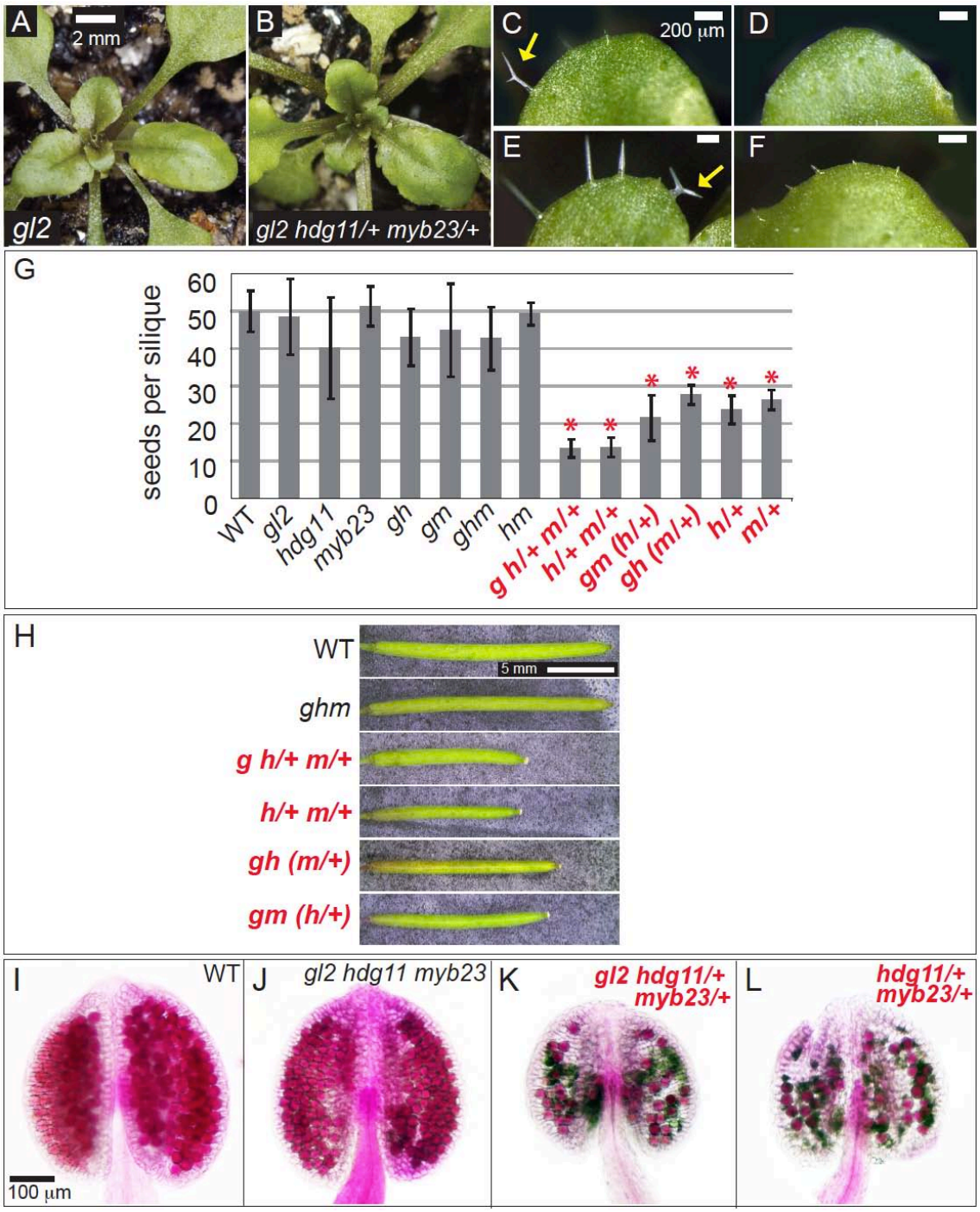

Supplemental Figure 5. Developmental defects of plants that are heterozygous for *hdg11-1* and/or *myb23-3*. (A-F) Trichome phenotypes of *gl2-5* plants heterozygous for *hdg11-1* and *myb23-3* are similar to those of the *gl2-5 hdg11-5* and *gl2-5 myb23-3* double mutants. **(A,C,E)** *gl2-5* plants exhibit both branched and unbranched trichomes on leaf margins. **(C,E)** Arrows indicate branched trichomes. **(B,D,F)** *gl2-5* plants heterozygous for *hdg11-1* and *myb23-3* exhibit leaves with fewer trichomes that are unbranched. **(G)** Seeds per silique were counted for 15 siliques from Col wild-type

(WT), *gl2-5* (*g*), *hdg11-1* (*h*), *myb23-3* (*m*), and double mutant and triple mutant combinations, as well as plants heterozygous for *hdg11-1* (*h/+*) and/or *myb23-3* (*m/+*). Standard deviations are indicated by error bars. Asterisks mark significant differences from WT (Two-tailed *t* test, $P < 0.0001$). **(H)** Mature siliques from Col WT, the triple mutant and various combinations of *hdg11-1/+ myb23-3/+* with and without the *gl2-5* mutation are shown. **(I-L)** Anthers were dissected from buds, fixed in Carnoy's solution, and stained as in (Peterson, 2010). Pollen was imaged with a 10x 0.3NA objective on an Olympus BX51WI microscope using a Canon T3i digital camera and DSLR Remote Pro software. **(I)** Col WT and **(J)** *gl2 hdg11 myb23* anthers exhibit viable pollen as indicated by magenta-red staining. In contrast, anthers from **(K)** *gl2-5 myb23-3/+ hdg11-1/+* and **(L)** *myb23-3/+ hdg11-1/+* plants show fewer viable pollen grains in addition to aborted pollen grains indicated by blue-green staining.

Reference

Peterson, R., Slovin, J.P, Chen, C. (2010). A simplified method for differential staining of aborted and non-aborted pollen grains. International Journal of Plant Biology **1**.

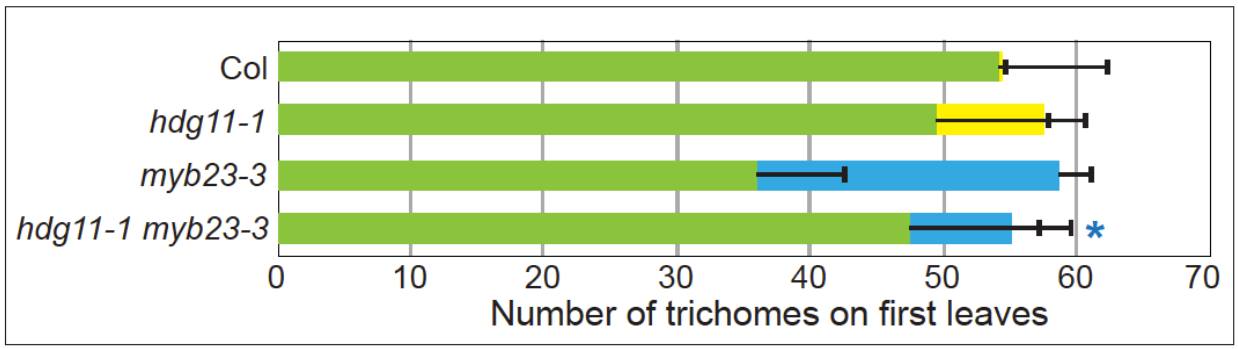

Supplemental Figure 6. Intermediate trichome phenotype of *hdg11-1 myb23-3* double mutants. Quantification of trichomes on first leaves. Green bars indicate the number of trichomes with 3-4 branches. Yellow bars show the number of trichomes with greater than four branches. Blue bars indicate the number of abnormal trichomes with fewer than three branches. Positive error bars indicate standard deviations for n $\geq$ 20 plants, and the blue asterisk points to a significant decrease in the number of abnormal trichomes with fewer than three branches in the *hdg11-1 myb23-3* double mutant in comparison to the *myb23-3* single mutant (Two-tailed *t* test, $P < 0.00001$).

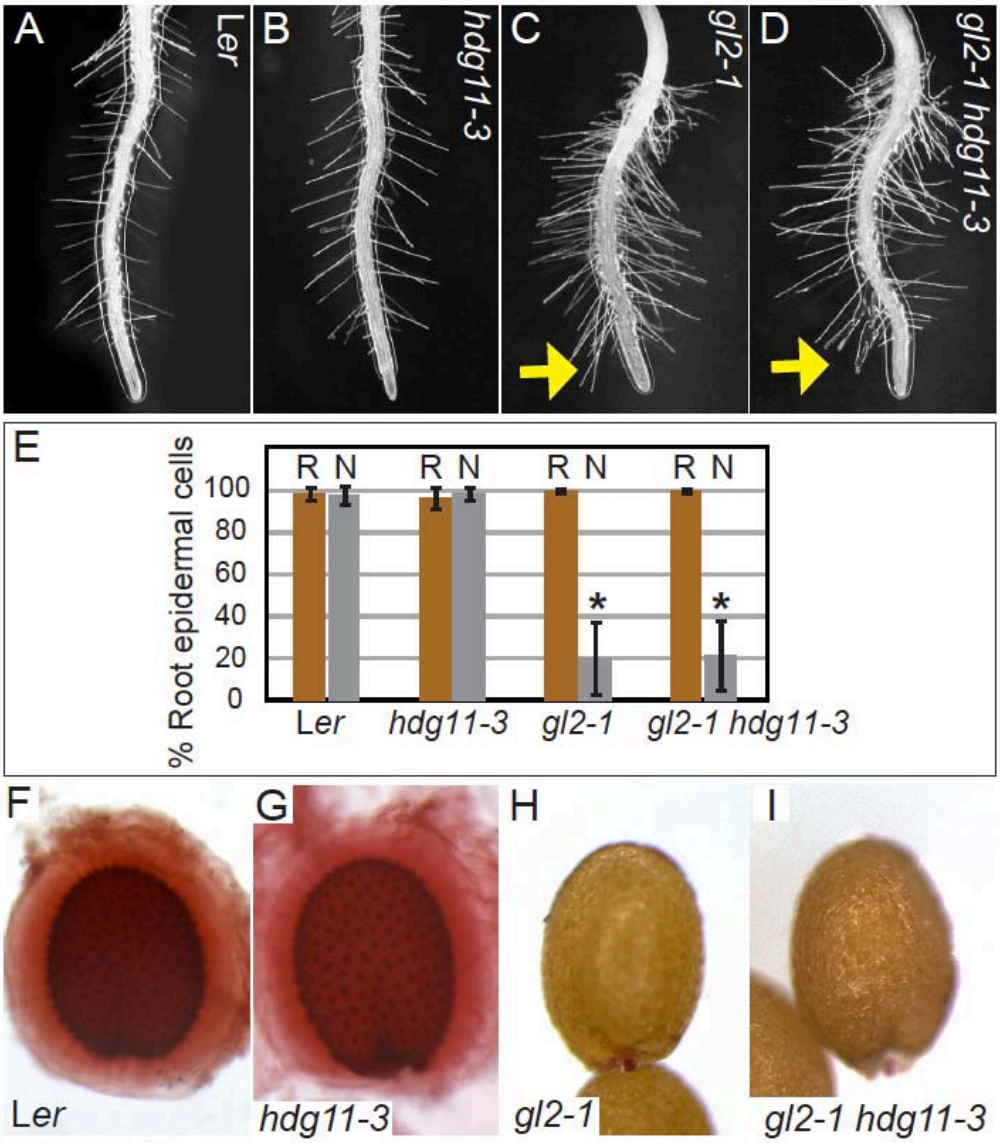

Supplemental Figure 7. Root hair density and seed mucilage phenotypes in the L*er* ecotype. (A) L*er* wild-type and **(B)** *hdg11-3* exhibit normal root hair formation in contrast to **(C)** *gl2-1* single and **(D)** *gl2-1 hdg11-3* double mutants, which display excess root hair formation. Yellow arrows indicate abnormal root hair formation near the tips of the roots in *gl2* mutants. **(E)** Quantification of root epidermal cells. Percentages of trichoblast cells in root hair cell files (**R** = brown bars), and atrichoblast cells in non root hair cell files (**N** = grey bars) are indicated (n $\geq$ 20). Asterisks mark significant differences from L*er* wild-type (Two-tiered *t* test, P > 0.0001). **(F-H)** Seeds were stained with ruthenium red to detect mucilage production upon imbibition. **(F)** L*er* wild-type and **(G)** *hdg11-3* seeds display mucilage in contrast to **(H)** *gl2-1* single and **(I)** *gl2-1 hdg11-3* double mutants which lack mucilage.

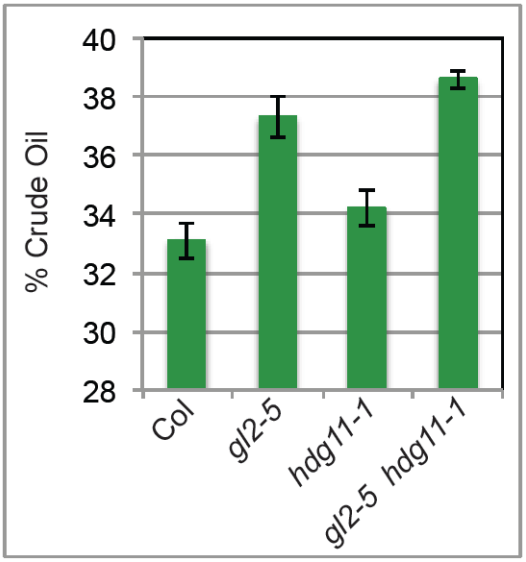

Supplemental Figure 8. Crude oil levels in *gl2* single and *gl2 hdg11* double mutant seeds are similar. In comparison to wild-type Col, *gl2* seeds exhibit higher percentages of crude oil. However, oil levels of *hdg11-1* seeds are similar to those of the wild type, and *gl2-5 hdg11-1* double mutant seeds are comparable to *gl2-5* seeds. A representative experiment from two biological replicates is shown with standard deviations for two 500-mg batches of seeds. The AOAC (Association of Analytical Communities) method 920.39 was used to perform quantitative oil analysis.

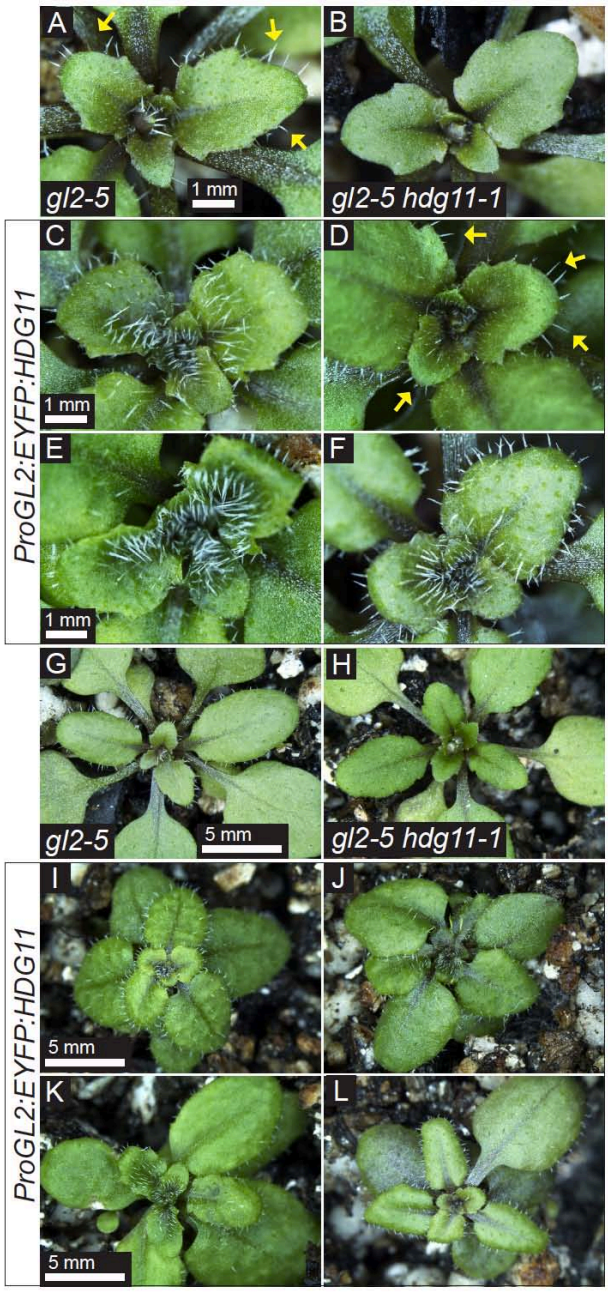

Supplemental Figure 9. Leaf and rosette phenotypes of *gl2* and *gl2 hdg11* mutant lines expressing *ProGL2:EYFP:HDG11*. **(A)** *gl2-5* rosette leaves exhibit trichomes at leaf margins (yellow arrows). **(B)** *gl2-5 hdg11-1* leaves appear largely devoid of trichomes. **(C-E)** *gl2-5* mutants and **(D,F)** *gl2-5 hdg11-1* mutants expressing *ProGL2:EYFP:HDG11* display increased trichome formation on leaves. The trichomes are typically unbranched. **(D)** *gl2-5 hdg11-1* mutants expressing *ProGL2:EYFP:HDG11* resemble *gl2-5* single mutants (yellow arrows), or **(F)** exhibit increased trichome differentiation phenotypes similar to those conferred by *ProGL2:EYFP:HDG11* in the *gl2-5* background **(C,E)**. **(G)** *gl2-5* and **(H)** *gl2-5 hdg11-1* rosettes are shown. **(I,K)** *gl2-5* mutants and **(J,L)** *gl2-5 hdg11-1* mutants transformed with *ProGL2:EYFP:HDG11* exhibit transient dwarf rosette phenotypes that appear either **(I,J)** symmetric or **(K,L)** notably asymmetric.

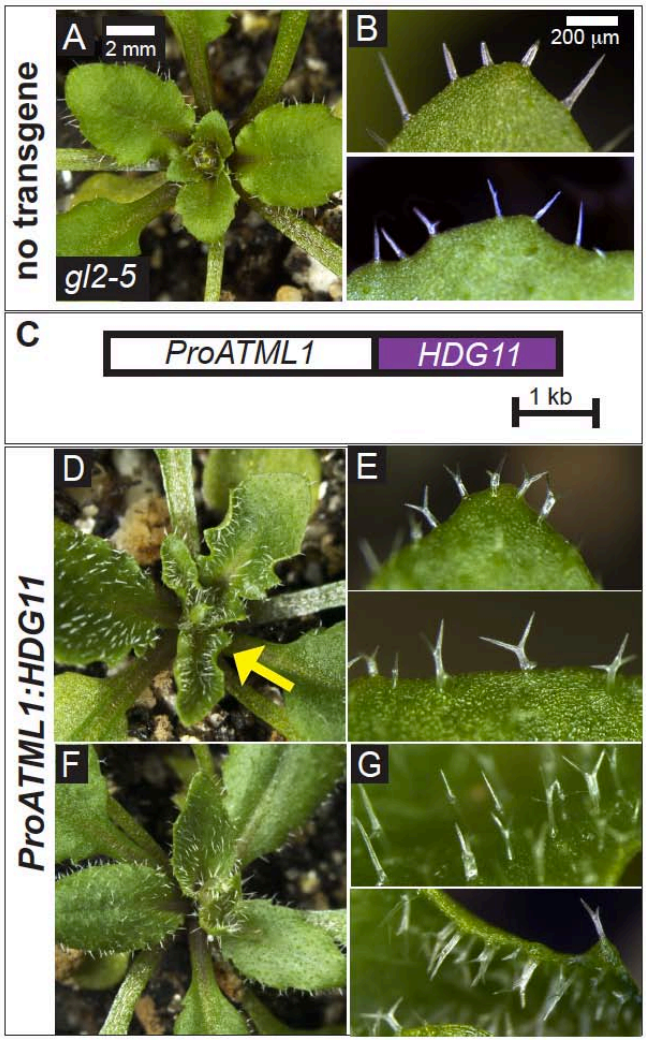

Supplemental Figure 10. Expression of *HDG11* under the *ATML1* epidermis-specific promoter induces trichome differentiation in *gl2* mutants. **(A,B)** *gl2-5* rosettes exhibit trichomes at the leaf margins but otherwise appear glabrous. **(C)** *ProATML1:HDG11* construct. **(D,F)** Two independent transformants that express *HDG11* under the *ATML* promoter are shown at the rosette stage. **(D)** Leaf curling (yellow arrow) and/or **(F)** pointy leaves were observed for several of the lines. **(E,G)** Magnification of leaf trichomes from *ProATML1:HDG11* transformants in comparison to **(B)** untransformed *gl2-5* plants indicates a partial rescue of the trichome phenotype.

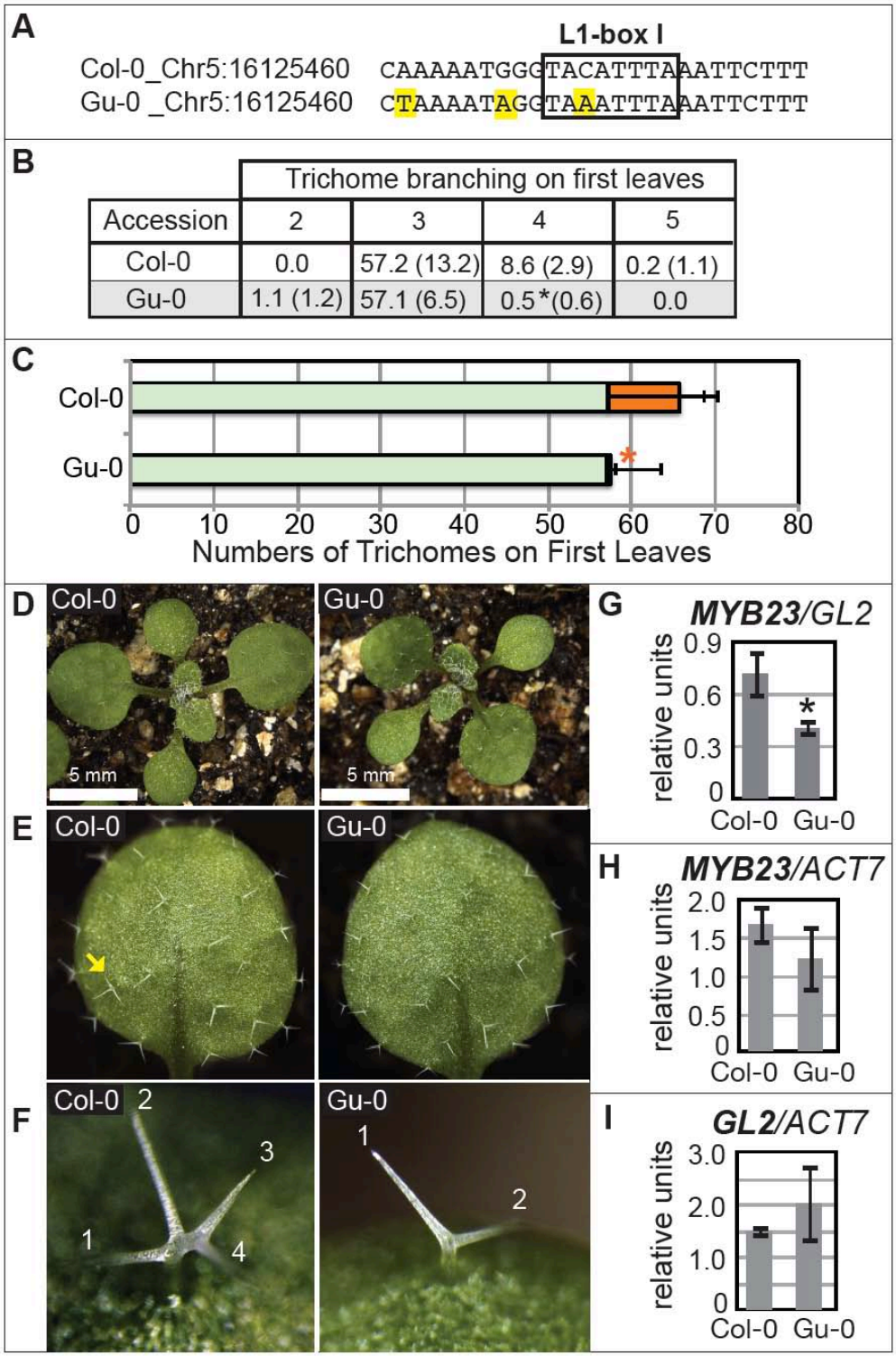

Supplemental Figure 11. A natural polymorphism in the *MYB23* L1-box I from the Gu-0 accession is correlated with reduced trichome branching. (A) Alignment of genomic sequence from the *MYB23* promoter in Col-0 and Gu-0 accessions. Single nucleotide polymorphisms (SNPs) are indicated for Gu-0 (yellow) and the L1-box 1 is boxed. **(B)** Quantification of trichomes and trichome branching on first leaves.

Percentages of trichomes with 2, 3, 4, or 5-branches are shown ($n \geq 20$) with standard deviations in parentheses. An asterisk marks a significant decrease in the number of 4-branched trichomes in Gu-0 in comparison to Col-0 (Two-tiered *t* test, $P < 0.00001$). **(C)** Graphical representation of the data in (B) illustrates numbers of 3-branched trichomes (green bars) and 4-branched trichomes (orange bars). **(D)** The rosettes of 10-day-old plants and **(E)** first leaves from Col-0 and Gu-0 accessions show similar leaf shapes. Yellow arrow marks a 4-branched trichome in Col-0. **(F)** Four-branched and 2-branched trichomes are shown for Col-0 and Gu-0, respectively. **(G-H)** Quantitative real-time PCR was performed with cDNA from 14-day-old seedling shoots. Data represent 3 biological replicates and normalized units are plotted on the Y-axis. Relative expression levels of **(G)** *MYB23* in comparison to *GL2*, and **(H)** *MYB23* and **(I)** *GL2* in comparison to the *ACT7* reference gene for the Col-0 and Gu-0 accessions. In (G), an asterisk marks a significant reduction of *MYB23* levels in Gu-0 in comparison to Col-0 (Two-tiered *t* test, $P < 0.05$).

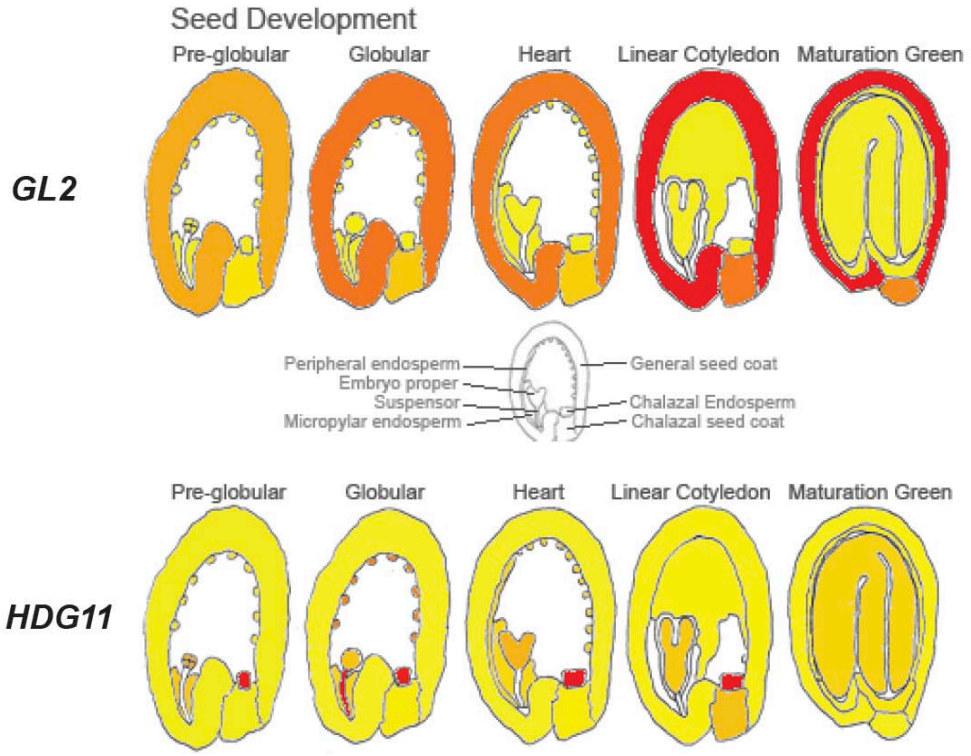

Supplemental Figure 12. Comparison of *GL2* and *HDG11* expression in the developing seed. These data are derived from the Bio-Analytic Resource (BAR) *Arabidopsis* eFP Browser (http://bar.utoronto.ca/efp/cgi-bin/efpWeb.cgi). Developing seeds from *Arabidopsis* ecotype Wassilewskija (Ws-0) were harvested from reproductive plants grown under continuous light. Subdomains of the immature seeds were separated by laser capture microdissection, followed by RNA extraction and amplification prior to hybridization on the GeneChip *Arabidopsis* ATH1 Genome Array (Affymetrix, Inc.). The data were generated by the Bob Goldberg and John J. Hanada labs (Le et al., 2010). Images are adapted from Meryl Hashimoto.

Reference

Le, B.H., Cheng, C., Bui, A.Q., Wagmaister, J.A., Henry, K.F., Pelletier, J., Kwong, L., Belmonte, M., Kirkbride, R., Horvath, S., Drews, G.N., Fischer, R.L., Okamuro, J.K., Harada, J.J., and Goldberg, R.B. (2010). Global analysis of gene activity during *Arabidopsis* seed development and identification of seed-specific transcription factors. Proc Natl Acad Sci U S A **107,** 8063-8070.

Supplemental Table 1. Pairwise alignments between the homeodomains from GL2/At1g79840 and each of the 15 other class IV HD-Zip family members. Protein-protein BLAST was performed with compositional score matrix (BLOSUM62) adjustment. The number of amino acids (aa) in each pairwise alignment is indicated. No gaps were found in the alignments. The HD-Zip derived sequences are sorted by % aa identity and % similarity to GL2/At1g79840. HDG11/At1g73360, HDG5/At5g46880 and PDF2/At4g04890 exhibit the largest degree of aa identity and similarity. HD-Zip transcription factors expressed in trichomes are indicated by an asterisk.

HD Domain	aa	% Identity	% Similarity
*HDG11/At1g73360	57	89	74
HDG5/At5g46880	59	88	75
PDF2/At4g04890	58	87	78
ATML1/At4g21750	57	85	65
*HDG2/At1g05230	56	85	70
*HDG12/At1g17920	57	84	68
ANL2/At4g00730	57	84	68
HDG4/At4g17710	59	83	71
HDG1/At3g61150	57	82	67
HDG7/At5g52170	57	80	61
HDG3/At2g32370	56	78	68
HDG9/At5g17320	57	75	65
HDG8/At3g03260	57	75	60
HDG10/At1g34650	50	74	54
HDG6/FWA/At4g25540	52	63	42

Supplemental Table 2. Trichome quantification on the first two leaves of *Arabidopsis* plants. See Figure 2U, Supplemental Figure 2M, Figures 3M, 3Q, 5T, 6H, and Supplemental Figure 6 for graphical representations of the data. Standard deviations for n≥20 plants are shown in parentheses. Significant differences for double mutants versus *gl2* single mutants are indicated by a single asterisk, significant differences between control and *HDG11* or *GL2* transgenes are indicated by double asterisks, and a significant difference between *myb23-3* and the *hdg11-1 myb23-3* double mutant is indicated by triple asterisks (Two-tiered *t* test, P < 0.00001).

Genotype	Ave. # trichomes 1 branch (*gl2*) 1-2 branch (*myb23*)	Ave. # trichomes 2-4 branch 3 branch (*myb23*)	Ave. # trichomes >4 branches	Ave. # total trichomes	Ave. % ectopic branched trichomes >4 branches	Ave. % branched trichomes >1 branch for *gl2* genotypes 1-2 branch (*myb23*)
Col wild-type	0	67.5 (7.5)	0.3 (0.9)	67.8 (7.4)	0.4 (1.3)	NA
hdg11-1	0	49.6 (9.6)	7.1 (3.0)	56.7 (11.0)	12.6 (5.3)	NA
gl2-5	6.5 (3.1)	0.8 (1.4)	0	7.3 (3.6)	0	11.0 (19.2)
gl2-5 hdg11-1	3.9 (3.4)	0*	0	3.9 (3.4)	0	0*
Col wild-type	0	68.8 (9.8)	NA	68.8 (9.8)	NA	NA
myb23-3	24.8 (5.6)	45.6 (14.7)	NA	70.3 (15.9)	NA	35.3 (8.0)
gl2-5 myb23-3	1.0 (1.2)	0*	0	1.0 (1.2)	0	0*
gl2-5	5.7 (3.3)	1.2 (0.9)	0	6.9 (3.3)	0	19.0 (13.0)
gl2-5 hdg11-1	3.4 (2.5)	0*	0	3.4 (2.5)	0	0*
gl2-5 myb23-3	1.4 (1.5)	0*	0	1.4 (1.5)	0	0*
gl2-1 hdg11-3 myb23-3	1.5 (1.6)	0*	0	1.5 (1.6)	0	0*
Ler wild-type	0	22.7 (2.2)	0.27 (0.46)	23.0 (2.2)	1.2 (2.0)	NA
hdg11-3	0	22.5 (4.0)	4.0 (3.0)	26.5 (5.1)	15.1* (11.3)	NA
gl2-1	2.9 (1.5)	1.9 (1.8)	0	4.8 (2.8)	0	39.6 (37.5)
gl2-1 hdg11-3	0.3* (0.9)	0*	0	0.3 (0.9)	0	0*
hdg11-1 + ProGL2:EYFP:hdg11Δ	0	55.3 (6.6)	10.9 (3.1)	66.2 (6.4)	16.5 (4.7)	NA
hdg11-1 + ProGL2:EYFP:HDG11	0	56.2 (8.1)	0.3** (0.5)	56.5 (8.1)	0.6** (0.9)	NA
gl2-5 + ProGL2:EYFP:hdg11Δ	5.5 (2.6)	2.0 (1.8)	0	7.5 (3.5)	0	26.7 (24)
gl2-5 + ProGL2:EYFP:HDG11	12.8** (3.9)	12.0** (3.8)	0	24.8** (3.9)	0	48.3 (15.3)
gl2-5 hdg11-1 + ProGL2:EYFP:hdg11Δ	0.4 (0.6)	0	0	0.4 (0.6)	0	0
gl2-5 hdg11-1 + ProGL2:EYFP:HDG11	7.8** (3.5)	6.1** (3.8)	0	13.9**(5.1)	0	43.9** (27.3)
hdg11-3 (control)	0	37.5 (10.9)	12.5 (4.3)	50.0 (12.6)	25.0 (8.6)	NA
hdg11-3 (no transgene sibling)	0	35.6 (8.7)	9.0 (3.3)	44.6 (10.3)	20.2 (7.4)	NA
hdg11-3 + proGL2::EYFP:GL2	0	73.2** (10.1)	2.0** (2.0)	75.2** (10.2)	2.7** (2.7)	NA

Genotype	**Ave. # trichomes 1 branch (*gl2*) 1-2 branch (*myb23*)**	**Ave. # trichomes 2-4 branch 3 branch (*myb23*)**	**Ave. # trichomes >4 branch**	**Ave. # total trichomes**	**Ave. % ectopic branched trichomes >4 branch**	**Ave. % branched trichomes >1 branch for *gl2* genotypes 1-2 branch (*myb23*)**
Col wild-type	0	54.1 (8.5)	0.3 (0.5)	54.4 (8.3)	0.5 (0.9)	NA
hdg11-1	0	49.5 (8.6)	8.1 (3.4)	57.5 (10.3)	14.1 (5.9)	NA
myb23-3	22.7 (2.8)	36.0 (6.9)	0	58.6 (7.5)	0	38.7 (4.8)
hdg11-1 myb23-3	7.7*** (2.2)	47.4 (12.3)	0	55.1 (12.4)	0	14.0 ***(4.0)

Supplemental Table 3. Quantification of trichoblast and atrichoblast hair cell files on roots. See Figure 4 and Supplemental Figure 7. Ten cells were counted in pairs of root hair (R) and non root hair (N) cell files. Standard deviations for n≥20 are shown in parentheses. Significant differences between wild-type and mutant are marked by a single asterisk. Significant differences between control and wild-type *HDG11* or *GL2* transgenes are indicated by a double asterisk (Two-tiered *t* test, P < 0.0001).

Genotype	% Trichoblast in R position	% Atrichoblast in N position
Col wild-type	97.5 (4.4)	98.8 (3.4)
hdg11-1	96.7 (4.8)	92.1 (8.8)
gl2-5	97.1 (5.5)	34.6* (15.0)
gl2-5 hdg11-1	95.8 (7.2)	30.8* (19.9)
myb23-3	97.1 (6.9)	92.9 (6.9)
gl2-5 myb23-3	96.5 (6.7)	43.0* (17.0)
Ler wild-type	98.0 (4.1)	97.5 (5.5)
hdg11-3	96.0 (5.9)	98.0 (4.1)
gl2-1	99.5 (2.2)	20.0* (18.0)
gl2-1 hdg11-3	99.5 (2.2)	21.5* (17.2)
hdg11-1 + ProGL2:EYFP:hdg11Δ	96.0 (6.0)	96.0 (6.8)
hdg11-1 + ProGL2:EYFP:HDG11	97.5 (4.4)	95.5 (6.9)
gl2-5 + ProGL2:EYFP:hdg11Δ	96.5 (5.9)	30.5 (18.2)
gl2-5 + ProGL2::EYFP:GL2	96.3 (5.8)	97.1** (5.5)
gl2-5 + ProGL2:EYFP:HDG11	95.4 (6.4)	62.1** (16.4)
gl2-5 hdg11-1 + ProGL2:EYFP:hdg11Δ	96.3 (6.0)	35.3 (19.0)
gl2-5 hdg11-1 + ProGL2:EYFP:HDG11	95.0 (8.3)	48.0 (20.1)

Supplemental Table 4. Oligonucleotides used in this study. Nucleotide bases shown in bold denote restriction sites used for cloning or changed bases from site-directed mutagenesis.

I. Primers for removing *Kpn*I and *Sal*I restriction sites from *HDG11* cDNA sequence using site-directed mutagenesis. Underlined bases show introduced mutation.	
Name	**5'-3' sequence**
HDG11_SalI_F(1602-32)	C ATG AAT GCT ATG GCA CTT **GTG GAC** ATG TTC ATG G
HDG11_SalI_R(1602-32)	C CAT GAA CAT GTC CAC AAG TGC CAT AGC ATT CAT G
HDG11_KpnI_F(1704-34)	GGA ATG GGA **GGC ACC** CAT GAG GGT GCA TTG C
HDG11_KpnI_R(1704-34)	G CAA TGC ACC CTC ATG GGT GCC TCC CAT TCC
HDG11_KpnI_F(2075-2107)	T GCT TCT CTA TC**G GTG CC**A GCG TCT TCA TCT CG
HDG11_KpnI_R(2075-2107)	CG AGA TGA AGA CGC TGG CAC CGA TAG AGA AGC A
II. Primers for amplification and cloning of *HDG11* cDNA in binary vector SR54	
HDG11_KpnI_F	GAAAGAG**GGTACC**AGAAGAAAGAGGGAAGAGAGC
HDG11_ SalI_R	GAAACATTAA**GTCGAC**AAAATGAGTTTCGTCGTCGGCG
III. Primers for sequence verification of *HDG11* cDNA in *ProGL2:EYFP:HDG11*	
HDG11_(804-23)_seq	CGT TAC CAT CGT CAC ACC GC
HDG11_(1223-45)_seq	TC CAA TGC ACA TCT CAC CGT TGG
HDG11_(1935-56)_seq	TCC AAG GTT ACT TGG GTT GAA C
HDG11_(2471-92)_seq	T GGA TCC AAT GCA ACA CAT AGC
B6_(EYFP)_seq	CAA GGA CGA CGG CAA CTA C
IV. Primers for cloning in pENTR™/D-TOPO (Start codons, italics; Stop codons, red)	
GL2_TOPO_F	CACC ***ATG*** TCA ATG GCC GTC GAC ATG
GL2_TOPO_R	**TCA TTA** GCA ATC TTC GAT TTG TAG ACT TC
HDG11_TOPO_F	CACC ***ATG*** AGT TTC GTC GTC GGC GTC GGC G
HDG11_TOPO_R	GTG **TCA** AGC TGT AGT TGA AGC TGT AGG
V. Primers for real-time PCR to monitor transcript levels of GL2, HDG11, and MYB23	
ACT7_PCR(94)_F	TCGCACATGTACTCGTTTCGCTTTC (amplifies 94 bp)
ACT7_PCR(94)_R	TCGAGAAGCAGCGAGAGAGAAAGATAGA
GL2_PCR_F	ATGAAGCTCGTCGGCATGAGTGGG (ampifies 106 bp) (Ishida et al., 2007)
GL2_PCR_R	TGGATTGCCACTGAGTTGCCTCTG (Ishida et al., 2007)
HDG11_RT(125)_F	TGGGGCTGATCGTTGGGTTACCA (amplifies 125 bp)
HDG11_RT(125)_R	TGCTTCTCTTCCCTTCCGGTGA
MYB23_RT(126)_F	CATCAGACTCCACAAGCTCCTCGG (amplifies 126 bp)
MYB23_RT(126)_R	TCTCCGAGACCAAGTTTCTTGCTGAG
VI. Primers for genotyping mutants	
GL2_F_112	ATGTCAATGGCCGTCGACATGTC (Wang et al., 2007)
GL2_R_1462	TCTCGCAGCTTCTCTAGTTCCG (Wang et al., 2007)
En8130 (3'outward) (*gl2-5*)	GAGCGTCGGTCCCCACACTTCTATAC (Baumann et al., 1998)
oAR283_hdg11-1_F	ATT CTA TCA CCG GAA GGG AAG (Roeder et al., 2012)
oAR284_hdg11-1_R	TGA AGA GAA AGA GAC ACC CAG (Roeder et al., 2012)
SLB1 (SAIL_LB1) (*hdg11-1*)	GCCTTTTCAGAAATGGATAAATAGCCT (Roeder et al., 2012)
oAR300_hdg11-3_F	GTG AAG ATC CTT ACT TTG ATG AT (Roeder et al., 2012)
oAR301_hdg11-3_R	TCA AGC TAT GCA AAA AGA TCA AA (Roeder et al., 2012)
myb23-3_SALK_018613_LP	CAC CGA ACA ACA AAA CAC ATG
myb23-3_SALK_018613_RP	TTT ACG TGG ACG TTT TTG CTC

LbB1 (for *myb23-3*)	GCG TGG ACC GCT TGC TGC AAC T
VII. Primers for sequencing *ProATML1* constructs in *pAR176* (Roeder et al., 2010)	
Name	**5'-3' sequence**
oAR204	CTT CCC TTT CTC CTA AGT TCC T
oAR424	GGA GAA AAA TAG AGA GAG ATA G
VIII. Primers for screening and sequencing inserts in *pAbAi* vector	
pAbAi_Seq_F	GTTCCTTATATGTAGCTTTCGACAT (ampifies 298 bp without insert and 323 with insert)
pAbAi_R	CAGAGCACATGCCTCGAGG
IX. Primers for L1-boxes from *MYB23* promoter (L1-boxes, bold; first L1-box out of three, underlined; mutations, lowercase)	
proMYB23_LI-box-I_F	C**TACATTTATACATTTATACATTTA**G
proMYB23_LI-box-I_R	TCGAC**TAAATGTATAAATGTATAAATGTA**GGTAC
proMYB23_mutLI-box-I_F	C**TACggTTATACggTTATACggTTA**G
proMYB23_mutLI-box-I_R	TCGAC**TAAccGTATAAccGTATAAccGTA**GGTAC
proMYB23_LI-box-II_F	C**TAAATGTGTAAATGTGTAAATGT**GG
proMYB23_LI-box-II_R	TCGAC**CACATTTACACATTTACACATTTA**GGTAC
proMYB23_mutLI-box-II_F	C**TAAccGTGTAAccGTGTAAccGT**G
proMYB23_mutLI-box-II_F	TCGAC**CACggTTACACggTTACACggTTA**GGTAC
X. Primers for construction of pGAD-T7 constructs for HD-Zip expression in yeast (Start codons, italics; Stop codons, red)	
GL2_747aa_EcoRI_F	GACAGG**GAATTC** *ATG* TCA ATG GCC GTC GAC ATG TCT TCC
GL2_231aa_BamHI_R	ATCGTC**GGATCCTCA** AGC CTG CAG GGG ATA GGG
HDG11_722aa_EcoR1_F	TAATTA**GAATTC** *ATG* AGT TTC GTC GTC GGC GTC GGC GG
HDG11_169aa_BamH1_R	TGTAG**GGATCCCTA** TTG CGA TAT CGG TCT TCC CAT GTA C
XI. Primers for construction of pGAD-T7 control construct for expression of GL2 (START + SAD) (Stop codons, red)	
GL2_253aa_EcoRI_F	GTCTTT**GAATTC** GAG AAG TCC CGT ATT GCC GAG ATT TC
GL2_747aa_BamHI_R	TGCTGT**GGATCCTCATCA** GCA ATC TTC GAT TTG TAG AC
XII. Primers for real-time PCR of ChIP DNA	
ACT7_ChIP_F	CGTTTCGCTTTCCTTAGTGTTAGCT
ACT7_ChIP_R	AGCGAACGGATCTAGAGACTCACCTTG
proCESA5_ChIP_F	GTATAGTCATCACTCAGGAGAC
proCESA5_ChIP_R	GACTCACTGAGTCTTTTTATCGG
proMYB23_ChIP_F	GGATCCACACAAGACTAAAATAC
proMYB23_ChIP_R	GCTATTCACATTTAGATTTTCCATC
XIII. Primers for deletion of L1-Box I in *ProMYB23:mGFP5-ER*	
ΔL1-box_F	CTTAAATTCTTTTTCACAAGATGTTTATAATG
ΔL1-box_R	GGTACCCATTTTTGTTGTATTTTAGTC
IX. Primers for sequencing *ProMYB23:mGFP5-ER*	
MYB23pro_2703_F	TCTAGAGTTTGGTATCACGG
MYB23pro_1836_F	TATTAGTATAGTTTGTTGTTCAAACGG
MYB23pro_seq_2082_R	TTCTTACATTTCATCTCATTGC
MYB23pro_3450_F	ACGGGTGTTAACACACACC

REFERENCES

Baumann, E., Lewald, J., Saedler, H., Schulz, B., and Wisman, E. (1998). Successful PCR-based reverse genetic screens using an En-1-mutagenised *Arabidopsis* thaliana population generated via single-seed descent. Theor Appl Genet **97,** 729-734.

Ishida, T., Hattori, S., Sano, R., Inoue, K., Shirano, Y., Hayashi, H., Shibata, D., Sato, S., Kato, T., Tabata, S., Okada, K., and Wada, T. (2007). *Arabidopsis* TRANSPARENT TESTA GLABRA2 is directly regulated by R2R3 MYB transcription factors and is involved in regulation of *GLABRA2* transcription in epidermal differentiation. Plant Cell **19,** 2531-2543.

Roeder, A.H., Cunha, A., Ohno, C.K., and Meyerowitz, E.M. (2012). Cell cycle regulates cell type in the *Arabidopsis* sepal. Development **139,** 4416-4427.

Roeder, A.H., Chickarmane, V., Cunha, A., Obara, B., Manjunath, B.S., and Meyerowitz, E.M. (2010). Variability in the control of cell division underlies sepal epidermal patterning in *Arabidopsis thaliana*. PLoS Biol **8,** e1000367.

Wang, S., Kwak, S.H., Zeng, Q., Ellis, B.E., Chen, X.Y., Schiefelbein, J., and Chen, J.G. (2007). *TRICHOMELESS1* regulates trichome patterning by suppressing *GLABRA1* in *Arabidopsis*. Development **134,** 3873-3882.